

Copper(I)–Olefin Complexes: The Effect of the Trispyrazolylborate Ancillary Ligand in Structure and Reactivity

Carmen Martín,[†] José María Muñoz-Molina,[†] Abel Locati,[§] Eleuterio Alvarez,[‡]
Feliu Maseras,[§] Tomás R. Belderrain,^{*,†} and Pedro J. Pérez^{*,†}

[†]Laboratorio de Catálisis Homogénea, Departamento de Química y Ciencia de los Materiales, Unidad Asociada al CSIC, Centro de Investigación en Química Sostenible (CIQSO), Campus de El Carmen s/n, Universidad de Huelva, 21007 Huelva, Spain, [§]Institute of Chemical Research of Catalonia (ICIQ), Avenida Paisos Catalans 16, 43007 Tarragona, Spain, and [‡]Instituto de Investigaciones Químicas, CSIC-Universidad de Sevilla, Avenida Américo Vespucio 49, 41092 Sevilla, Spain

The spectroscopic and structural characteristics and the relative reactivity of several $\text{Tp}^{\text{Ms}}\text{Cu}$ -olefin (olefin = ethylene, **1**, 1-hexene, **2**, allyl ethyl ether, aee, **3**, cyclohexene, **4**, and styrene, **5**) complexes bearing the bulky hydrotris(3-mesitylpyrazolyl)borate ligand have been examined. Experimental data, including an unusual high-field chemical shift in the ^1H and ^{13}C NMR spectra, and DFT theoretical calculations support the proposal that the copper–olefin linkage is mainly sustained by σ -donation, lacking a substantial degree of π -back-donation.

Introduction

The interaction between copper(I) centers and ethylene is crucial in plants.^{1,2} In addition, copper(I)–alkene complexes have been used as catalyst precursors and proposed as the resting state in several copper-catalyzed reactions.³ It is well known that such binding is reversible, and therefore, most copper(I)–ethylene complexes are labile. The first stable copper(I) ethylene complex, $\text{Tp}^*\text{Cu}(\eta^2\text{-C}_2\text{H}_4)$ ($\text{Tp}^* = [\text{HB}(3,5\text{-Me}_2\text{pz})_3]$, Scheme 1a), was reported by Thompson and co-workers.⁴ Although stable in the solid state toward ethylene loss,⁵ the coordinated olefin was easily removed under vacuum. The most stable systems described to date usually contain anionic ligands (Scheme 1) such as iminophosphinamide (b),⁶ β -diketiminato (c),⁷ the highly fluorinated 1,3,5-triazapentadienyl (d),⁸ tris(pyrazolyl)borate

$[\text{HB}\{3,5\text{-(CF}_3)_2\text{pz}\}]$ (e),⁹ or $[\text{MeB}(3\text{-(CF}_3\text{)pz})_3]$ ¹⁰ (f) ligands. The latter compounds have been described as air-stable solids, which do not lose ethylene under reduced pressure.

The copper–olefin bonds of the above and other complexes have been rationalized by means of the Dewar–Chatt–Duncanson model.¹¹ The ancillary ligands bonded to the metal center affect the relative energy of the σ - and π -type metal orbitals and subsequently exert a certain influence on the metal–olefin bond. Thus, the π -back-bonding interaction can be enhanced with strongly Lewis-basic ancillary ligands, whereas weakly donating (electron-withdrawing) ligands will decrease such interaction, lowering the energy of the empty Cu 4s and 4p orbitals. In the latter case, a stronger metal–olefin σ -interactions arises.¹² Usually, the donating properties of the ancillary ligands L_n can be evaluated by means of IR studies with the corresponding carbonyl complexes $\text{L}_n\text{Cu}(\text{CO})$.

In the past decade, we have described the use of Tp^xCuL ($\text{Tp}^x =$ trispyrazolylborate ligand,¹³ L (leaving group) = olefin, acetonitrile) complexes as catalysts for several reactions involving olefins as the substrate: cyclopropanation,¹⁴ aziridination,¹⁵ epoxidation,¹⁶ atom transfer radical addition,¹⁷

*To whom correspondence should be addressed. E-mail: perez@dqcm.uhu.es (P.J.P), trodri@dqcm.uhu.es (T.R.B.).

(1) Khan, N.A. *Ethylene Action in Plants*; Springer-Verlag: Berlin, 2006.

(2) (a) Schaller, G. E.; Bleecker, A. B. *Science* **1995**, *270*, 1809–1811. (b) Rodríguez, F. I.; Esch, J. J.; Hall, A. E.; Binder, B. M.; Schaller, G. E.; Bleecker, A. B. *Science* **1999**, *283*, 996–998. (c) Ecker, J. R. *Science* **1995**, *268*, 667–675, and references therein.

(3) Pérez, P. J.; Díaz-Requejo, M. M. *Copper Organometallics*. In *Comprehensive Organometallic Chemistry III*, Vol. 2; Elsevier: Amsterdam, 2007.

(4) Thompson, J. S.; Harlow, R. L.; Whitney, J. F. *J. Am. Chem. Soc.* **1983**, *105*, 3522–3527.

(5) (a) Dias, H. V. R.; Wu, J. *Eur. J. Inorg. Chem.* **2008**, 509–522, and references therein. (b) Dias, H. V. R.; Lovely, C. J. *Chem. Rev.* **2008**, *108*, 3223–3238.

(6) Straub, B. F.; Eisentrager, F.; Hofmann, P. *Chem. Commun.* **1999**, 2507–2508.

(7) Dai, X.; Warren, T. H. *Chem. Commun.* **2001**, 1998–1999.

(8) Dias, H. V. R.; Singh, S.; Flores, J. A. *Inorg. Chem.* **2006**, *45*, 8859–8861.

(9) Dias, H. V. R.; Lu, H.-L.; Kim, H.-J.; Polach, S. A.; Goh, T. K. H. H.; Browning, R. G.; Lovely, C. J. *Organometallics* **2002**, *21*, 1466–1473.

(10) Dias, H. V. R.; Wang, X.; Diyabalanage, H. V. K. *Inorg. Chem.* **2005**, *44*, 7322–7324.

(11) Wang, X.-S.; Zhao, H.; Li, Y.-H.; Xiong, R.-G.; You, X.-Z. *Top. Catal.* **2005**, *35*, 43–61.

(12) Sullivan, R. M.; Liu, H.; Smith, D. S.; Hanson, J. C.; Osterhour, D.; Ciraolo, M. F.; Grey, C. P.; Martin, J. D. *J. Am. Chem. Soc.* **2003**, *125*, 11065–11079.

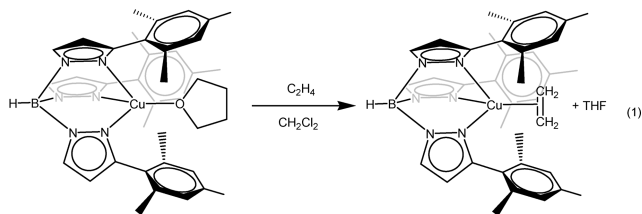
(13) (a) Trofimenko, S. *Scorpionates: The Coordination of Polypyrazolylborate Ligands*; Imperial College Press: London, 1999. (b) Pettinari, C. *Scorpionates II: Chelating Borate Ligands*; Imperial College Press: London, 2008.

(14) (a) Díaz-Requejo, M. M.; Belderrain, T. R.; Trofimenko, S.; Pérez, P. J. *J. Am. Chem. Soc.* **2001**, *123*, 3167–3168. (b) Díaz-Requejo, M. M.; Caballero, A.; Belderrain, T. R.; Nicasio, M. C.; Trofimenko, S.; Pérez, P. J. *J. Am. Chem. Soc.* **2002**, *124*, 978–983.

and atom transfer radical addition and cyclization.¹⁸ Since the formation of olefin adducts has been proposed along the catalytic cycles in those transformations, we decided to investigate the stability of such complexes by preparing a series of compounds of general formula $\text{Tp}^{\text{Ms}}\text{Cu}(\text{olefin})$ and performing a spectroscopic, structural, and reactivity study. A second factor that was taken into account is the well-known ability of the substituents located at the distal-to-boron position in these ligands, which exert a fundamental role in the definition of the catalytic pocket around the metal center. Because of this, we chose the hydrotris(3-mesitylpyrazolyl)borate (Tp^{Ms}) as the ligand on the basis of the steric effect of the Ms groups, which provides the biggest cone angles known for $\text{Tp}^{\text{X}}\text{M}$ complexes.¹³

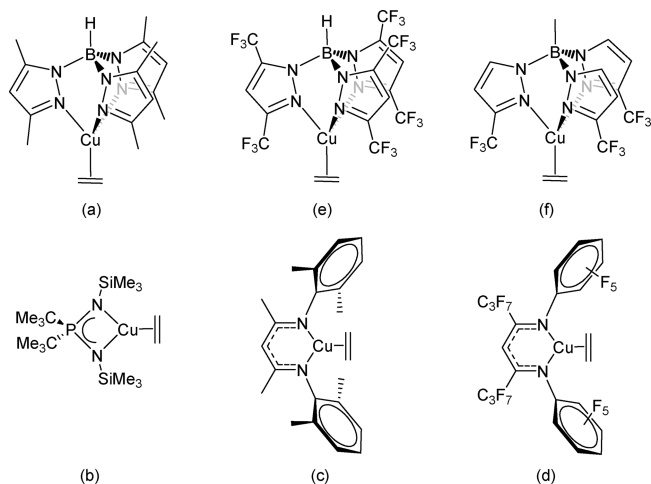
Results and Discussion

Synthesis and Characterization of the Ethylene Complex $\text{Tp}^{\text{Ms}}\text{Cu}(\text{C}_2\text{H}_4)$ (1**).** When ethylene was bubbled through a solution of Tolman's complex¹⁹ $\text{Tp}^{\text{Ms}}\text{Cu}(\text{THF})$ (Tp^{Ms} = hydrotris(3-mesityl)pyrazolylborate) in dichloromethane for 1 h, a white crystalline solid came out of the solution upon addition of diethyl ether. This compound has been identified as $\text{Tp}^{\text{Ms}}\text{Cu}(\text{C}_2\text{H}_4)$, **1** (eq 1), on the basis of ^1H and ^{13}C NMR data, IR data, elemental analysis, and X-ray crystallography. This compound is remarkably stable, in a similar manner to the already mentioned fluorinated hydrotris(pyrazolyl)borate copper complexes:⁵ solid samples of **1** were stable under air for days, and when exposed to reduced pressure, ethylene loss was not observed.



Importantly, no free ethylene was detected in the solutions of **1** by ^1H NMR spectroscopy, even at +70 °C, assessing the high stability of this complex. The ^1H NMR resonance of the ethylene protons appeared as a sharp singlet at δ 3.03 (C_6D_6 , 298 K) or 2.72 (CDCl_3 , 298 K) shifted to higher field than the ethylene signals reported for the majority of copper(I)-olefin complexes.⁵ For instance, Thompson's complex⁴ $\text{Tp}^*\text{Cu}(\text{C}_2\text{H}_4)$ showed the corresponding peak at a higher chemical shift, δ 4.41 ppm (in CD_2Cl_2). Some authors have attributed the upfield shift of the ^1H NMR resonance of ethylene protons of copper(I) adducts to the increased shielding caused by the

Scheme 1. Stable Copper–Ethylene Complexes



copper-to-ethylene π -back-donation.²⁰ However, collected data did not support this proposal for the case of **1**.

The electronic properties of the Tp^{Ms} ligands can be estimated using the $\nu(\text{CO})$ frequencies^{5b,21} of the carbonyl adducts $\text{Tp}^{\text{X}}\text{Cu}(\text{CO})$. The values for the Tp^* and Tp^{Ms} derivatives have been reported as 2056 and 2079 cm^{-1} , respectively. If there were a correlation between the chemical shift of coordinated-ethylene protons and the electron density at the metal center, the chemical shift of such hydrogen nuclei for **1** should appear at a higher chemical shift than $\text{Tp}^*\text{Cu}(\text{C}_2\text{H}_4)$, that is, the opposite of the experimental observations. Therefore, we believe that the observed upfield shift of the ethylene resonances of **1** is better, and correctly, explained as a consequence of the anisotropy generated by the π -systems of the mesityl aromatic rings.²² A similar effect was found in the ^{13}C NMR spectra: the ethylene carbons resonated at δ 77.4 (C_6D_6 , 298 K) with an upfield shift of 46 ppm compared to free ethylene (δ 123.5 ppm). That chemical shift is slightly different than expected by comparison with experimental and calculated values in other copper complexes containing poor electron donor trispyrazolylborate ligands.²³ Moreover, the $^1J_{\text{CH}}$ coupling constant value of 161 Hz suggests a sp^2 -character of the C_2H_4 carbons in **1**. This constant for free ethylene is 156 Hz,²⁴ from which we can estimate that π -back-bonding in **1** is quite weak.

The structure of the molecules of **1** was confirmed by a X-ray single-crystal diffraction study. This compound crystallizes in the triclinic space group $P\bar{1}$. When data were acquired at 173 K, the double carbon–carbon bond distance, $\text{C}(37)\text{--}\text{C}(38)$, was found to be 1.299(8) Å, shorter than that for free ethylene (1.3369(16) Å).²⁵ A similar situation has been described by Dias et al. for the complex $[\text{HB}(3\text{--}(\text{CF}_3), 5\text{--}(\text{C}_6\text{H}_5)\text{pz})_3]\text{Cu}(\text{C}_2\text{H}_4)$,⁹ where a 1.30(1) Å distance was found for coordinated $\text{C}=\text{C}$. This observation was explained in terms of the existence of disorder of the ethylene unit, with the ethylene group in these adducts placed in a pocket with a significant amount of vibrational/rotational freedom. In our case, when a second set of data was collected at 100(2) K, the $\text{C}=\text{C}$ distance of coordinated ethylene was found to be

(15) Mairena, M. A.; Díaz-Requejo, M. M.; Belderrain, T. R.; Nicasio, M. C.; Trofimenko, S.; Pérez, P. J. *Organometallics* **2004**, *23*, 253–256.

(16) Díaz-Requejo, M. M.; Belderrain, T. R.; Pérez, P. J. *Chem. Commun.* **2000**, 1853–1854.

(17) Muñoz-Molina, J. M.; Caballero, A.; Díaz-Requejo, M. M.; Trofimenko, S.; Belderrain, T. R.; Pérez, P. J. *Inorg. Chem.* **2007**, *46*, 7725–7730.

(18) Muñoz-Molina, J. M.; Belderrain, T. R.; Pérez, P. J. *Adv. Synth. Catal.* **2008**, *350*, 2365–2372.

(19) Schneider, J. L.; Carrier, S. M.; Ruggiero, C. E.; Young, V. G., Jr.; Tolman, W. B. *J. Am. Chem. Soc.* **1998**, *120*, 11408–11418.

(20) Hertwig, R. H.; Koch, W.; Schroeder, D.; Schwarz, H.; Hrusak, J.; Schwerdtfeger, P. *J. Phys. Chem.* **1996**, *100*, 12253–12260.

(21) (a) Fujisawa, K.; Ono, T.; Ishikawa, Y.; Amir, N.; Miyashita, Y.; Okamoto, K.; Lehnert, N. *Inorg. Chem.* **2006**, *45*, 1698–1713. (b) Mairena, M. A.; Urbano, J.; Carbajo, J.; Maraver, J. J.; Alvarez, E.; Díaz-Requejo, M. M.; Pérez, P. J. *Inorg. Chem.* **2007**, *46*, 7428–7435.

(22) Abraham, R. J.; Canton, M.; Griffiths, L. *Magn. Reson. Chem.* **2001**, *39*, 421–431.

(23) Kazi, A. B.; Dias, H. V. R.; Tekarli, S. M.; Morello, G. R.; Cundari, T. R. *Organometallics* **2009**, *28*, 1826–1831.

(24) Friebolin, H. *Basic One- and Two-Dimensional NMR Spectroscopy*; VCH: Cambridge, 1992.

(25) Bartell, L. S.; Roth, E. A.; Hollowell, C. D.; Kuchitsu, K.; Young, J. E., Jr. *J. Chem. Phys.* **1965**, *42*, 2683–2686.

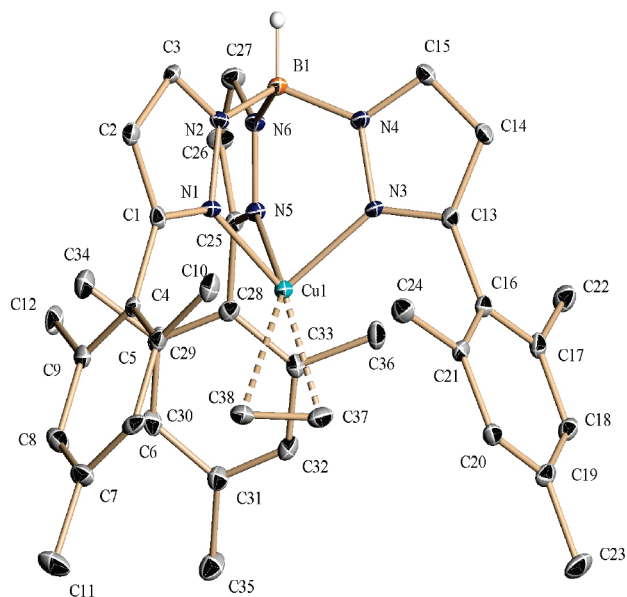


Figure 1. Molecular structure of $\text{Tp}^{\text{Ms}}\text{Cu}-(\text{C}_2\text{H}_4)$, **1** (30% displacement ellipsoids; hydrogen atoms have been omitted except for that bound to the boron atom).

1.345(6) Å, very similar but longer than that for the free molecule (1.3369(16) Å),²⁵ in good agreement with the observed $^1J_{\text{CH}}$ coupling constant. As observed in Figure 1, the ethylene molecule coordinates to copper(I) in a typical η^2 -fashion. The distances for Cu(1)–C(37) and Cu(1)–C(38), 2.034(4) and 2.029(4) Å, respectively, fall in the range (1.93–2.07 Å) previously observed for related complexes.^{5a} As found for other structures with the $\text{Tp}^{\text{Ms}}\text{Cu}$ core,¹⁹ the mesityl rings lie orthogonal to their respective pyrazolyl rings, providing a sort of pocket with aromatic walls, i.e., a “nest” to accommodate the alkene ligand. Due to the steric pressure of the mesityl groups, complex **1** displays a mononuclear nature, similar to that described for the parent complex $\text{Tp}^{\text{Ms}}\text{Cu}(\text{THF})$ ¹⁹ and in contrast with other copper complexes containing $\text{Tp}^{\text{R,R'}}$ ligands ($\text{R} = \text{R}' = \text{H}, \text{CH}_3, \text{or Ph}$; $\text{R} = \text{tBu}, \text{R}' = \text{H or CH}_3$), which preferred the dinuclear $[\text{Tp}^{\text{R,R'}}\text{Cu}]_2$ geometry.

Synthesis and Characterization of the Olefin Complexes $\text{Tp}^{\text{Ms}}\text{Cu}(\text{olefin})$ (olefin = 1-hexene, **2; allyl ethyl ether (aee), **3**; cyclohexene, **4**; styrene, **5**).** In order to expand the study to other olefins with different electronic and steric properties, we have prepared a series of olefin complexes upon addition of an excess of the corresponding olefin to a solution of $\text{Tp}^{\text{Ms}}\text{Cu}(\text{THF})$ in dichloromethane. Following this procedure, complexes $\text{Tp}^{\text{Ms}}\text{Cu}(\text{1-hexene})$ (**2**), $\text{Tp}^{\text{Ms}}\text{Cu}(\text{aee})$ (**3**), $\text{Tp}^{\text{Ms}}\text{Cu}(\text{cyclohexene})$ (**4**), and $\text{Tp}^{\text{Ms}}\text{Cu}(\text{styrene})$ (**5**) were isolated (eq 2) and characterized by ^1H and ^{13}C NMR, IR, and elemental analysis, as well as by X-ray crystallography in the case of **2** and **4**.



| olefin | complex |
|-------------------------|----------|
| 1-hexene | 2 |
| allyl ethyl ether (aee) | 3 |
| cyclohexene | 4 |
| styrene | 5 |

Table 1 displays NMR data for complexes **1–5**. Signals due to the coordinated $\text{CH}_2=\text{CH}$ protons of **2** and **3**

Table 1. Selected NMR Data of $\text{Tp}^{\text{Ms}}\text{Cu}(\text{olefin})$ Complexes^a

| $\text{Tp}^{\text{Ms}}\text{Cu}[\text{olefin}]$ | ^1H | ^{13}C |
|--|--|---|
| $\text{Tp}^{\text{Ms}}\text{Cu}(\text{C}_2\text{H}_4)$, 1 ^b | $\text{CH}_2_{\text{olef}}$ 3.08 (5.28) ^c | C_{olef} 77.4 (123.5) |
| $\text{Tp}^{\text{Ms}}\text{Cu}(\text{1-hexene})$, 2 ^b | CH_{olef} 4.00 (5.80) $\text{CH}_2_{\text{olef}}$ 3.28 and 3.21 (4.96 and 4.92) | CH_{olef} 101.5 (137.9) $\text{CH}_2_{\text{olef}}$ 78.5 (114.4) |
| $\text{Tp}^{\text{Ms}}\text{Cu}(\text{aee})$, 3 ^d | CH_{olef} 3.66 (5.91) $\text{CH}_2_{\text{olef}}$ 2.92 and 2.78 (5.27 and 5.17) | CH_{olef} 93.6 (134.4) $\text{CH}_2_{\text{olef}}$ 70.2 (116.4) |
| $\text{Tp}^{\text{Ms}}\text{Cu}(\text{cyclohexene})$, 4 ^b | CH_{olef} 4.70 (5.66) | CH_{olef} 99.4 (127.3) |
| $\text{Tp}^{\text{Ms}}\text{Cu}(\text{styrene})$, 5 ^b | CH_{olef} 5.18 (6.55) $\text{CH}_2_{\text{olef}}$ 3.75 and 3.56 (5.59 and 5.00) | CH_{olef} 98.0 (135.8) $\text{CH}_2_{\text{olef}}$ 77.9 (111.3) |

^a Chemical shift in ppm. ^b C_6D_6 . ^c Free olefin proton's chemical shift between brackets. CDCl_3 . ^d CD_2Cl_2 .

appeared significantly shifted upfield when compared to the resonances of the free olefins (1-hexene or aee) and other α -olefin copper complexes.²⁶ Accordingly, the chemical shift of the C_α ($\text{CH}_2=\text{CH}$) and C_β ($\text{CH}_2=\text{CH}$) olefin carbon also emerged shifted to lower frequencies compared to free olefins. Yet the rest of the protons resonances corresponding to both 1-hexene and aee were shifted, probably due, as proposed for **1**, to the anisotropy caused by the π -systems of the mesityl rings. For instance, the methylene $\text{CH}_2=\text{CH}-\text{CH}_2$ protons in **2** resonated at δ 2.42 and 1.73 ppm (3.95 ppm in free 1-hexene), whereas the methylene OCH_2CH_3 in **3** appeared at δ 2.81 and 2.71 (3.47 ppm in free aee).

Complex **2** was isolated as good X-ray quality colorless crystals from CH_2Cl_2 solutions. The solid-state structure is shown in Figure 2 (data collected at 173 K). The C=C distance of coordinated 1-hexene, C(37)–C(38), determined for **2**, 1.278(7) Å, is quite similar to that reported for $[\text{Cu}(\text{dien})(\text{1-hexene})](\text{BPh}_4)$ by Floriani and co-workers²⁷ and to the average values of the free olefin.²⁸ As in other α -olefin complexes,²⁹ the Cu(I) atom is located closer to the unsubstituted carbon atom (C_β) (Cu(1)–C(37), 2.002(4) Å) than the substituted carbon atom (C_α) (Cu(1)–C(38), 2.095(5) Å). This difference found for the two Cu–C distances is in good accord with the chemical shifts of the olefin protons and carbons in the ^1H and ^{13}C NMR spectra already discussed.

Complexes **2** and **3** have been found to be very stable, lacking olefin loss under vacuum. However, a different behavior has been observed with the copper complexes containing the bulkier olefins styrene and cyclohexene. Because of this, complexes **4** and **5** had to be isolated in the presence of excess olefin. Both complexes also showed different NMR spectra when compared with **1–3**. Thus, the ^1H NMR spectrum of **4** in C_6D_6 showed $\text{CH}_{\text{olefin}}$ protons as a broad singlet centered at 4.57 ppm. Similarly, the

(26) (a) Allen, J. J.; Barron, A. R. *Dalton Trans.* **2009**, 878–890. (b) Braunecker, W. A.; Pintauer, T.; Tsarevsky, N. V.; Kickelbick, G.; Matyjaszewski, K. *J. Organomet. Chem.* **2005**, 690, 916–924.

(27) Pasquali, M.; Floriani, C.; Gaetani-Manfredotti, A.; Chiesi-Villa, A. *Inorg. Chem.* **1979**, 18, 3535–3542.

(28) The more reliable overage determination of the double-bond length for free olefin was retrieved from the Cambridge Structural Database. See: Allen, F. H. *Acta Crystallogr. Sect. B: Struct. Sci.* **2002**, 58, 380–388.

(29) Pintauer, T.; Matyjaszewski, K. *Coord. Chem. Rev.* **2005**, 249, 1155–1184.

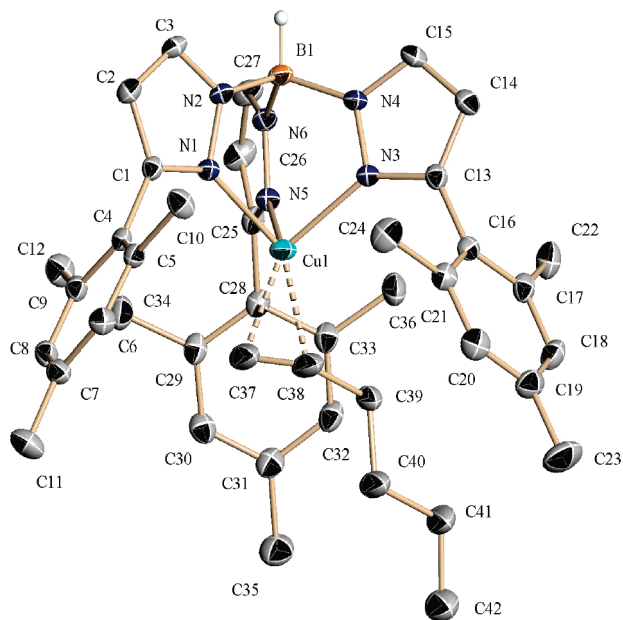


Figure 2. Molecular structure of $\text{Tp}^{\text{Ms}}\text{Cu}(1\text{-hexene})$, **2** (30% displacement ellipsoids; hydrogen atoms have been omitted except for that bound to the boron atom).

resonances corresponding to the olefinic protons in the ^1H NMR spectrum of **5** in C_6D_6 appeared at δ 5.18 (C_βH , dd, $J_{\text{HH}} = 15.3$ Hz, $J_{\text{HH}} = 9.4$ Hz), 3.75 ($\text{C}_\alpha\text{H}_2$, d, $J_{\text{HH}} = 9.5$ Hz), and 3.56 ($\text{C}_\alpha\text{H}_2$, d, $J_{\text{HH}} = 15.2$ Hz). Although these resonances are also upfield shifted with respect to those of the free olefins, the degree of shifting was not as pronounced as in the case of complexes **1–3**. The origin of this difference may lie in the steric interaction of cyclohexene or styrene with the mesityl rings in $\text{Tp}^{\text{Ms}}\text{Cu}(\text{cyclohexene})$ and $\text{Tp}^{\text{Ms}}\text{Cu}(\text{styrene})$, weakening the copper–olefin interaction. Since back-bonding in these copper–olefin adducts is relatively weak, a facile rotation about the Cu–olefin bond is expected. Indeed, the rotational barrier for the olefin ligand has been calculated by VT ^1H NMR (through coalescence of the signals of mesityl aromatic CH protons at -40 °C) as $\Delta G^\ddagger = 10.9(3)$ kcal mol $^{-1}$. This value is similar to that reported by Warren and co-workers for the β -diketiminato copper(I) styrene complex.⁷

The structure of **4** was confirmed by X-ray crystallography, an Ortep drawing being shown in Figure 3. The bond distances Cu(1)–C(37) and Cu(1)–C(42), 2.1146(14) and (2.1110(13) Å, in **4** are larger than those found in **1**, in good agreement with the already proposed weaker metal–olefin bond in **4** as inferred from NMR studies. The observed elongation could be explained as the result of steric interactions between the olefin and the mesityl groups. Indeed, these Cu–carbon distances are longer than those reported by Thompson and Whitney³⁰ for the dinuclear cyclohexene adduct 1-chloro-2-(η^2 -cyclohexene)- μ -[hydrotris(1-pyrazolyl)borato- $N:N',N''$]dicopper(I), 2.039(2) and 2.022(2) Å, or Stamp and Dieck³¹ for the monomeric compound (cyclohexene)[glyoxalbis(2-diisopropylphenylimine)-trifluoromethanesulfonate]copper(I), 2.00(2) and 2.06(2) Å. In addition, as expected for a negligible copper-to-olefin

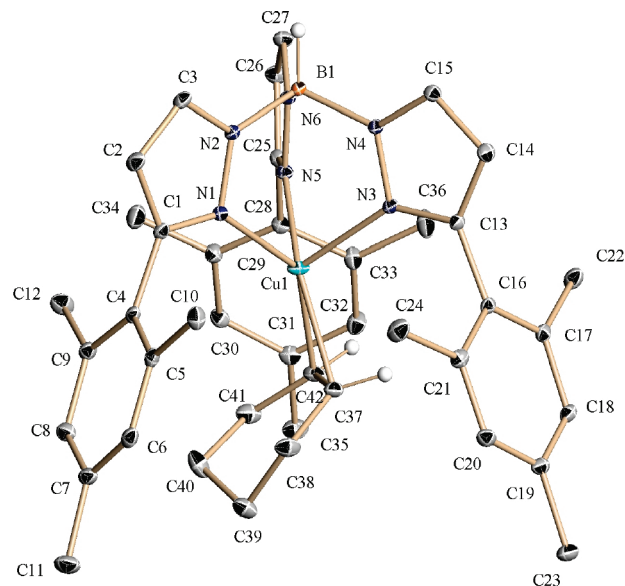
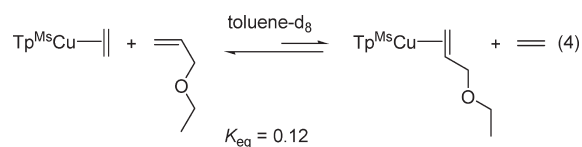


Figure 3. Molecular structure of $\text{Tp}^{\text{Ms}}\text{Cu}(\text{cyclohexene})$, **4** (30% displacement ellipsoids; hydrogen atoms have been omitted except for that bound to the boron atom).

back-bonding, the C=C double bond distance of the coordinated cyclohexene of C(37)–C(42) (1.368(2) Å) is ca. 0.03 Å longer than that reported for the free olefin, 1.335(3) Å.³²

Olefin Exchange Reactions. In order to compare the stability of the olefin adducts, we decided to investigate the olefin exchange reactions and determine the exchange equilibrium constants. Thus, when 1 equiv of styrene was added to a solution of $\text{Tp}^{\text{Ms}}\text{Cu}(\text{C}_2\text{H}_4)$ in a NMR scale (C_6D_6), no exchange was observed after 5 h, and therefore we could not estimate the exchange equilibrium constant. Consequently, ethylene complex **1** is much more thermodynamically favored over the styrene adduct **5**. However, when 1 equiv of aee, a less bulky olefin compared with styrene, was added to a solution of $\text{Tp}^{\text{Ms}}\text{Cu}(\text{C}_2\text{H}_4)$, the formation of $\text{Tp}^{\text{Ms}}\text{Cu}(\text{aee})$ (eq 4) was observed by NMR spectroscopy along with the appearance of free ethylene. After 5 h, an equilibrium mixture of **1** and **3** in the ratio of 2.55:1 was attained. On the basis of this ratio and the concentration of both olefins, the equilibrium constant K_{eq} has been estimated as 0.12(1) at room temperature: again, the ethylene adduct **1** seems to be more stable than the aee complex, **3**.



In an attempt to evaluate the effect of electronic factors, we have carried out the exchange reactions of $\text{Tp}^{\text{Ms}}\text{Cu}(1\text{-hexene})$ (**2**) with aee, since 1-hexene and aee are similar from a steric point of view but differ substantially in electronic density. When 1 equiv of aee was added to a solution of **2**,

(30) Thompson, J. S.; Whitney, J. F. *Acta Crystallogr.* **1984**, C40, 756–759.

(31) Stamp, L.; Dieck, H. T. *Inorg. Chim. Acta* **1987**, 129, 107–114.

(32) Chiang, J. F.; Bauer, S. H. *J. Am. Chem. Soc.* **1969**, 91, 1898–1901.

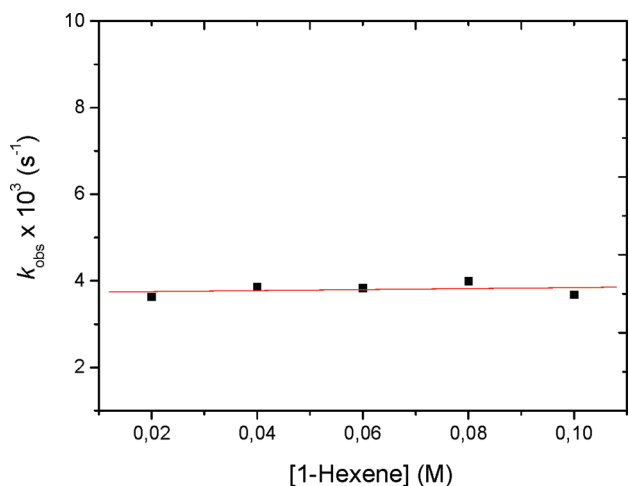
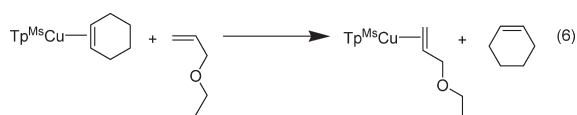
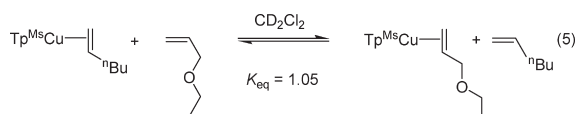


Figure 4. Influence of the entering olefin concentration on k_{obs} in the exchange reaction of **3** and 1-hexene.

a ca. 1:1 mixture of **2** and **3** was observed after the equilibrium was reached (eq 5). Finally, $\text{Tp}^{\text{Ms}}\text{Cu}(\text{cyclohexene})$ (**4**) reacted with 1 equiv of aee to afford compound **3** quantitatively (eq 6).

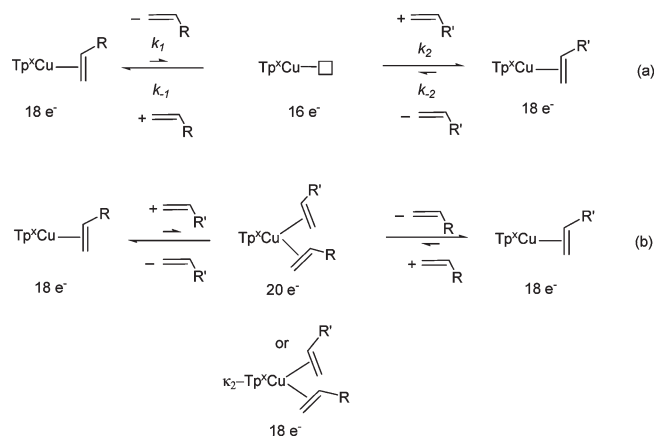


From experimental data, we can conclude at this stage that the relative stability of the different $\text{Tp}^{\text{Ms}}\text{Cu}(\text{olefin})$ complexes is mainly governed by steric factors. The bulkier olefins such as cyclohexene or styrene were easily replaced by smaller olefins, whereas in the cases of similar size (e.g., 1-hexene and allyl ethyl ether) the equilibrium mixture contains equimolar amounts of both complexes. The ethylene complex seemed to be the most stable, probably due to the lowest size that allows a better packing of the olefin between the aromatic walls. Indeed, when ethylene is bubbled through a solution of $\text{Tp}^{\text{Ms}}\text{Cu}(\text{styrene})$, **5**, the equilibrium is totally shifted to the formation of the ethylene adduct, **1** (eq 7). In order to check if **1** was stable in the presence of styrene even in the absence of free ethylene, N_2 was bubbled through the above solution. After 48 h, the ^1H NMR spectrum of the mixture remained unchanged with **1** as the only observable olefin adduct.



Kinetic Studies of the Exchange of $\text{Tp}^{\text{Ms}}\text{Cu}(\text{aee})$ with 1-Hexene. The observed exchange process may occur by a dissociative (Scheme 2a) or an associative mechanism (Scheme 2b). In the dissociative mechanism, the rate-determining step would be the formation of a 16-electron species, the olefin concentration having no effect on k_{obs} . In

Scheme 2. Possible Olefin Exchange Mechanisms



the associative mechanism a pentacoordinated 20e^- species (or alternatively an unlikely $18\text{-electron } \kappa^2\text{-Tp}^{\text{x}}\text{Cu}(\text{aee})(1\text{-hexene})$) would be formed, and in this case a certain effect of the olefin concentration should be expected.

With the aim of elucidating the actual mechanism we have carried out a kinetic study of the exchange reaction of $\text{Tp}^{\text{Ms}}\text{Cu}(\text{aee})$ with different amounts of 1-hexene. Monitoring the reaction by ^1H NMR at room temperature provided no useful information since equilibrium was reached immediately. However, at 0°C the process was slow enough to carry out the desired study. Thus, to five solutions of $\text{Tp}^{\text{Ms}}\text{Cu}(\text{aee})$ (0.02 M) in 0.7 mL of CD_2Cl_2 , variable amounts of 1-hexene (1 to 5 equiv) were added. The values of k_{obs} at those different olefin concentrations were obtained by first-order linear plots of $\ln([\text{3}]_t/[\text{3}]_0 - [\text{3}]_e)$ vs time (see Supporting Information). As shown in Figure 4, k_{obs} remained almost unchanged with the increase of entering olefin concentration, in good accord with the existence of a dissociative mechanism (Scheme 2a). Therefore, the global equilibrium is controlled by the ratio of k_1 vs k_{-2} , being shifted to the olefin with the less steric influence.

DFT Calculations for the Exchange Reactions. We have carried out DFT studies to evaluate the steric influences on the $\text{Tp}^{\text{Ms}}\text{Cu}$ backbone after ligation of ethylene, 1-hexene, allyl ethyl ether, and cyclohexene and, therefore, on the stabilities of the corresponding olefin adducts. The B3LYP functional applied is sufficient to describe the problem at hand, because it properly describes the stability trends observed experimentally in the exchange reactions. The strongest coordination free energy corresponds to ethylene, followed by allyl ethyl ether, 1-hexene, and cyclohexene, which have weaker binding, by 2.6, 3.5, and 8.7 kcal mol^{-1} , respectively, relative to ethylene (see Supporting Information). The calculation seems to exaggerate the energy differences, but the order of stabilities is reproduced. The experimental equilibrium constant of 2.55 in favor of the ethylene coordination with respect to aee is reflected in a computed free energy difference of 2.6 kcal mol^{-1} . The smallest free energy difference of 0.9 kcal mol^{-1} between AEE and 1-hexene corresponds to the almost 1:1 experimental equilibrium, while the largest difference of 6.1 kcal mol^{-1} between aee and cyclohexene corresponds to the experimental case where the reactions is completely shifted. The computed energy values clearly confirm that the weakest coordination corresponds to the bulkier olefin, cyclohexene, whereas the strongest one corresponds to the smallest olefin, the ethylene. The adducts of linear olefins,

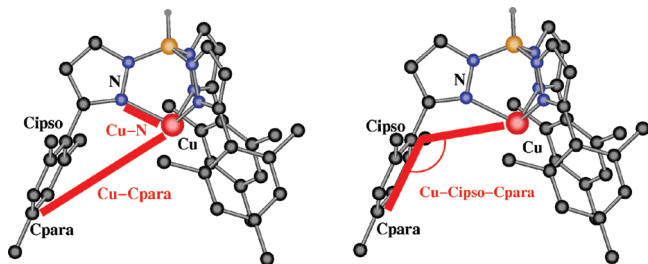


Figure 5. Cu–N and C–Cu distances and C–C–Cu angle employed to evaluate the steric distortion of the $\text{Tp}^{\text{Ms}}\text{Cu}$ fragment. Hydrogen atoms have been removed for clarity.

Table 2. Values of the Cu–N Distances (Å) for the $\text{Tp}^{\text{Ms}}\text{Cu}(\text{olefin})$ Complexes (see Figure 4)

| complex | average | Cu–N distances | | |
|---|---------|----------------|-------|-------|
| $\text{Tp}^{\text{Ms}}\text{Cu}(\text{C}_2\text{H}_4)$, 1 | 2.155 | 2.069 | 2.081 | 2.314 |
| $\text{Tp}^{\text{Ms}}\text{Cu}(\text{1-hexene})$, 2 | 2.166 | 2.156 | 2.078 | 2.264 |
| $\text{Tp}^{\text{Ms}}\text{Cu}(\text{AEE})$, 3 | 2.162 | 2.152 | 2.072 | 2.262 |
| $\text{Tp}^{\text{Ms}}\text{Cu}(\text{cyclohexene})$, 4 | 2.218 | 2.114 | 2.102 | 2.437 |

Table 3. Values of the Cu– $\text{C}_{\text{para-mesityl}}$ Distances (Å) (see Figure 4)

| complex | average | C–Cu distances | | |
|---|---------|----------------|-------|-------|
| $\text{Tp}^{\text{Ms}}\text{Cu}(\text{C}_2\text{H}_4)$, 1 | 5.754 | 5.677 | 5.680 | 5.905 |
| $\text{Tp}^{\text{Ms}}\text{Cu}(\text{1-hexene})$, 2 | 5.860 | 5.832 | 5.795 | 5.953 |
| $\text{Tp}^{\text{Ms}}\text{Cu}(\text{AEE})$, 3 | 5.857 | 5.827 | 5.792 | 5.952 |
| $\text{Tp}^{\text{Ms}}\text{Cu}(\text{cyclohexene})$, 4 | 5.960 | 5.901 | 5.912 | 6.091 |

Table 4. Values of the Cu– $\text{C}_{\text{ipso}}-\text{C}_{\text{para-mesityl}}$ Angles (deg) (see Figure 4)

| complex | average | $\text{C}_{\text{ipso}}-\text{C}_{\text{para-mesityl}}-\text{Cu}$ angles | | |
|---|---------|--|-------|-------|
| $\text{Tp}^{\text{Ms}}\text{Cu}(\text{C}_2\text{H}_4)$, 1 | 120.3 | 120.6 | 119.8 | 120.4 |
| $\text{Tp}^{\text{Ms}}\text{Cu}(\text{1-hexene})$, 2 | 122.3 | 122.0 | 123.1 | 121.9 |
| $\text{Tp}^{\text{Ms}}\text{Cu}(\text{AEE})$, 3 | 122.6 | 123.2 | 122.0 | 121.9 |
| $\text{Tp}^{\text{Ms}}\text{Cu}(\text{cyclohexene})$, 4 | 123.6 | 125.4 | 120.8 | 124.7 |

allyl ethyl ether and 1-hexene, show similar stabilities, which again points toward the lack of a significant electronic effect in the interaction of the olefin with copper.

DFT Calculations for the Structures. All structures can be viewed like an upside-down nest shaped by the $\text{Tp}^{\text{Ms}}\text{Cu}$ backbone (Figure 5). The steric effects should show up in distortions of this nest, which we evaluated with the three magnitudes shown in Figure 5: the Cu–N and Cu– $\text{C}_{\text{para-mesityl}}$ distances and the Cu– $\text{C}_{\text{ipso}}-\text{C}_{\text{para-mesityl}}$ angles, which are collected in Tables 2, 3, and 4.

As can be seen in Tables 2–4, the results of these calculations always indicate the same trend: two extreme values, corresponding to ethylene and cyclohexene, and two intermediate values close to each other for 1-hexene and aee. The bulkier olefin cyclohexene induced a higher degree of aperture of the $\text{Tp}^{\text{Ms}}\text{Cu}$ nest, whereas for the ethylene adduct this pocket is the smallest. It is also worth mentioning that 1-hexene and allyl ethyl ether provoked a similar distortion, in spite of their differences in electronics.

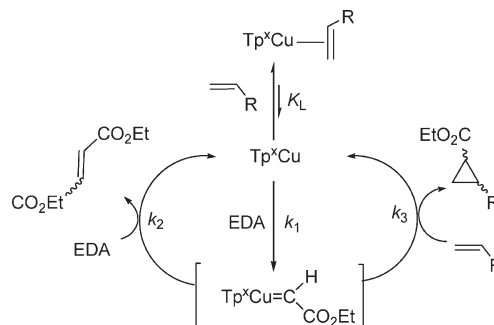
The bond distances corresponding to the olefin coordination to the metal are not so informative in terms of steric/electronic terms, because both factors are involved. In any case, the calculated $\text{C}_{\text{olefin}}-\text{Cu}$ distances (Table 5) in the cyclohexene complex are longer than for the rest of the complexes studied, in good agreement with the X-ray data. Finally, the calculated C=C bond distances (Table 5) show

Table 5. Calculated $\text{C}_{\text{olefin}}-\text{Cu}$ Distances (Å)^a

| complex | C–Cu distance | C–C distance |
|---|---------------|--------------|
| $\text{Tp}^{\text{Ms}}\text{Cu}(\text{C}_2\text{H}_4)$, 1 | 2.079/2.08 | 1.376 |
| $\text{Tp}^{\text{Ms}}\text{Cu}(\text{1-hexene})$, 2 | 2.141/2.081 | 1.376 |
| $\text{Tp}^{\text{Ms}}\text{Cu}(\text{AEE})$, 3 | 2.120/2.077 | 1.375 |
| $\text{Tp}^{\text{Ms}}\text{Cu}(\text{cyclohexene})$, 4 | 2.149/2.143 | 1.376 |

^a Values calculated using the B3LYP functional.

Scheme 3. Olefin Cyclopropanation Catalytic Cycle Proposed for $\text{Tp}^{\text{X}}\text{Cu}$ As the Catalyst



that there are no electronic differences for the four olefins in the type of interaction with the metal, being almost identical.

Effect of Olefin Coordination in $\text{Tp}^{\text{Ms}}\text{Cu}$ -Catalyzed Olefin Cyclopropanation. Our group has previously reported³³ the catalytic capabilities of the complex $\text{Tp}^{\text{Ms}}\text{Cu}$ for several catalytic transformations involving the transfer of the carbene moiety $:\text{CHCO}_2\text{Et}$ from ethyl diazoacetate ($\text{N}_2\text{CHCO}_2\text{Et}$, EDA), including the olefin cyclopropanation reaction.¹⁴ We proposed (Scheme 3) the existence of an equilibrium involving the olefin adducts $\text{Tp}^{\text{X}}\text{Cu}(\text{olefin})$ as the resting state of the catalyst.^{14b} Such equilibrium controls the amount of the real catalytic species, $\text{Tp}^{\text{X}}\text{Cu}$, in the reaction mixture. Hence, if the equilibrium constant of formation of the olefin adduct, K_L , were very high, a very stable adduct would be formed and the reaction rate would significantly decrease.

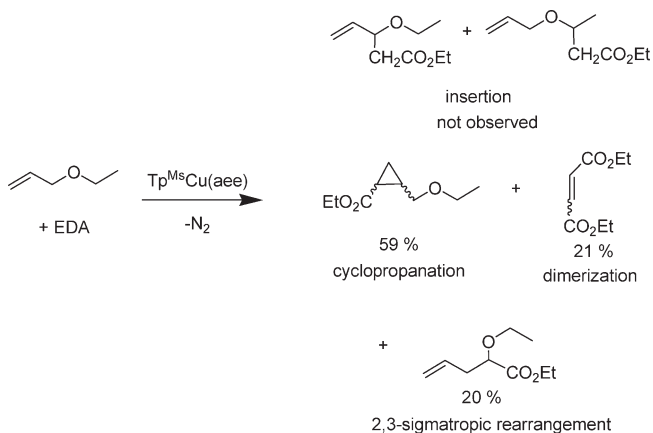
When complex $\text{Tp}^{\text{Ms}}\text{Cu}(\text{THF})$ was employed as the catalyst for the reaction of allyl ethyl ether and ethyl diazoacetate, at room temperature, no consumption of the diazo compound was observed after 24 h. This is in contrast with the well-known capabilities of this compound to induce the cyclopropanation of styrene in quantitative yield and with high reaction rates (250 h^{-1}).^{14b} The use of the isolated complex $\text{Tp}^{\text{Ms}}\text{Cu}(\text{aee})$ as catalyst precursor did not make any difference, until the reaction was performed at 70°C . Under those conditions, EDA was consumed and the mixture of products shown in Scheme 4 was detected by ^1H NMR. In addition to the cyclopropane derivative,³⁴ the carbene group was, copper-mediated, inserted into the C–H bonds vicinal to the oxygen atoms as well as to the oxygen atom to give an ylide intermediate that underwent a 2,3-sigmatropic rearrangement.³⁵

(33) Díaz-Requejo, M. M.; Pérez, P. J. *J. Organomet. Chem.* **2005**, *690*, 5441–5450.

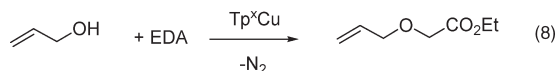
(34) (a) Díaz-Requejo, M. M.; Belderrain, T. R.; Nicasio, M. C.; Trofimenko, S.; Pérez, P. J. *J. Am. Chem. Soc.* **2002**, *124*, 896–897. (b) Caballero, A.; Díaz-Requejo, M. M.; Belderrain, T. R.; Nicasio, M. C.; Trofimenko, S.; Pérez, P. J. *Organometallics* **2003**, *22*, 4145–4150.

(35) (a) Doyle, M. P.; McKervey, M. A.; Ye, T. *Modern Catalytic Methods for Organic Synthesis with Diazo Compounds*; John Wiley & Sons: New York, 1998.

Scheme 4. Reaction of Allyl Ethyl Ether with Ethyl Diazoacetate Using $\text{Tp}^{\text{Ms}}\text{Cu}(\text{ace})$ As the Catalyst



The low catalytic activity of $\text{Tp}^{\text{Ms}}\text{Cu}(\text{ace})$ reminded us of the results reported by our group in a study on the insertion of the carbene fragment $:\text{CHCO}_2\text{Et}$ into the OH bonds of unsaturated alcohols using several $\text{Tp}^{\text{x}}\text{Cu}$ complexes as the catalyst.³⁶ When allyl alcohol was employed as the substrate, the ether derived from the insertion reaction (eq 8) was obtained in almost quantitative yields for an array of catalysts, with the exception of $\text{Tp}^{\text{Ms}}\text{Cu}$, for which the yield was low at room temperature. Such anomalous behavior can now be explained in terms of the formation of an allylic alcohol copper complex that should be quite stable, precluding olefin decoordination and therefore blocking diazo compound coordination and further metalcarbene formation.



Conclusion. We have collected experimental as well as theoretical data relevant to the nature of the copper–olefin bond in a series of $\text{Tp}^{\text{Ms}}\text{Cu}(\text{olefin})$ complexes. We have found that the impact of steric factors is more relevant in the stability of these complexes than that of the electronic ones (small olefins, as ethylene, afford more stable complexes than styrene or cyclohexene). We have also shown that extracting conclusions about the copper–olefin bonding only from chemical shifts of the olefin protons and carbons in ^1H or ^{13}C NMR spectra can be misleading, since the substituents on the other ligands (in our case, the mesityl rings of the Tp^{Ms} ligand) may have an influence on those data.

Experimental Section

General Methods. All reactions and manipulations were carried out under an oxygen-free nitrogen atmosphere with standard Schlenk techniques. All substrates were purchased from Aldrich. Solvents were dried and degassed before use. $\text{Tp}^{\text{Ms}}\text{Cu}(\text{THF})$ ¹⁹ complex was prepared according to the reported method. NMR spectra were recorded on a Varian Mercury 400 MHz spectrometer using deuterated solvents. IR data were collected in a Varian Scimitar 1000 Fourier transform IR spectrophotometer. Elemental analyses were performed in Unidad de Análisis Elemental at the Instituto de Investigaciones Químicas, CSIC-Universidad de Sevilla.

(36) Morilla, M. E.; Molina, M. J.; Díaz-Requejo, M. M.; Belderrain, T. R.; Nicasio, M. C.; Trofimenko, S.; Pérez, P. J. *Organometallics* **2003**, *22*, 2914–2918.

Synthesis of $\text{Tp}^{\text{Ms}}\text{Cu}[\text{C}_2\text{H}_4]$ (1). This complex was synthesized by bubbling C_2H_4 for 30 min through a dichloromethane solution of $\text{Tp}^{\text{Ms}}\text{Cu}(\text{THF})$ (0.11 g, 0.16 mmol). Complexes were obtained as crystalline solids in the solution in 80% yield. Anal. Calcd for $\text{BC}_{41}\text{H}_{50}\text{N}_6\text{O}_{10}\text{Cu} \cdot \frac{1}{3}\text{CH}_2\text{Cl}_2$: C 66.91, H 6.44, N 12.22. Found: C 67.18, H 6.52, N 12.06. IR (KBr): $\nu(\text{B}-\text{H})$ 2440 cm^{-1} , $\nu(\text{C}=\text{C})$ 1518 cm^{-1} . ^1H NMR (400 MHz, CDCl_3): δ 7.78 (d, $J = 2.1$ Hz, 3H), 6.82 (s, 6H), 6.03 (d, $J = 2.3$, 3H), 2.72 (s, 4H), 1H), 2.26 (s, 9H), 1.91 (s, 18H). ^{13}C NMR (100 MHz, CDCl_3): δ 151.04 (*Cq* pyrazol), 137.79 (*Cq* mesityl), 137.49 (*Cq* mesityl), 134.91 (CH pyrazol), 131.77 (*Cq* mesityl), 127.79 (CH mesityl), 104.74 (CH pyrazol), 77.43 (CH_2 olefin), 21.3 (CH_3), 20.57 (CH_3).

General Synthesis Procedure for $\text{Tp}^{\text{Ms}}\text{Cu}[\text{olefin}]$. To a stirred solution of $\text{Tp}^{\text{Ms}}\text{Cu}(\text{THF})$ (0.1 g, 0.16 mmol) in CH_2Cl_2 (10 mL) was added the olefin (30 mmol). The mixture was stirred for 1 h at room temperature. After the removal of the volatiles under reduced pressure, a white solid was obtained in quantitative yield. The complex was purified by recrystallization. All complexes were obtained as crystalline solids in 80% yield.

$\text{Tp}^{\text{Ms}}\text{Cu}(\text{1-hexene})$ (2). Anal. Calcd for $\text{BC}_{41}\text{H}_{50}\text{N}_6\text{O}_{10}\text{Cu} \cdot \frac{3}{2}\text{CH}_2\text{Cl}_2$: C 61.94, H 6.52, N 9.97. Found: C 62.41, H 6.41, N 10.17. IR (KBr): $\nu(\text{B}-\text{H})$ 2441 cm^{-1} , $\nu(\text{C}=\text{C})$ 1520 cm^{-1} . ^1H NMR (400 MHz, C_6D_6): δ 7.76 (d, $J = 2.1$ Hz, 3H), 6.79 (s, 6H), 5.99 (d, $J = 2.3$, 3H), 4.00 (dddd, $J = 15.0$, 9.6, 8.7, 3.5 Hz, 1H), 3.28 (d, $J = 8.3$, 1H *cis*), 3.21 (d, $J = 15$, 1H *trans*), 2.16 (s, 9H), 1.12 (s, 18H), 1.07–0.88 (m, 2H), 0.8 (m, 3H), 0.6–0.55 (m, 2H), 0.37–0.32 (m, 2H). ^{13}C NMR (100 MHz, C_6D_6): δ 151.64 (*Cq* pyrazol), 137.82 (*Cq* mesityl), 137.33 (*Cq* mesityl), 135.34 (CH pyrazol), 132.37 (*Cq* mesityl), 128.08 (CH mesityl), 104.95 (CH pyrazol), 101.65 (CH olefin), 78.59 (CH_2 olefin), 33.52 (3CH_2), 21.03 (CH_3), 20.79 (CH_3), 14.25 (CH_3).

$\text{Tp}^{\text{Ms}}\text{Cu}(\text{ace})$ (3). Anal. Calcd for $\text{BC}_{41}\text{H}_{50}\text{N}_6\text{O}_{10}\text{Cu} \cdot \frac{1}{4}\text{CH}_2\text{Cl}_2$: C 67.15, H 6.90, N 11.39. Found: C 66.97, H 6.83, N 11.34. IR (KBr): $\nu(\text{B}-\text{H})$ 2425 cm^{-1} , $\nu(\text{C}=\text{C})$ 1516 cm^{-1} . ^1H NMR (400 MHz, CD_2Cl_2): δ 7.81 (d, $J = 2.1$ Hz, 3H), 6.84 (s, 6H), 6.03 (d, $J = 2.3$, 3H), 3.66 (dddd, $J = 15.0$, 9.6, 8.7, 3.5 Hz, 1H), 2.92 (d, $J = 8.3$, 1H *cis*), 2.81 (qd, $J = 9.1$, 7.01 Hz, 1H), 2.78 (d, $J = 15$, 1H *trans*), 2.71 (dq, $J = 9.1$, 7.01 Hz, 1H), 2.42 (dd, $J = 9.6$, 3.6, 1H), 2.25 (s, 9H), 1.90 (s, 18H), 1.73 (t, $J = 9.6$ Hz, 1H), 0.89 (t, $J = 7.01$ Hz, 3H). ^{13}C NMR (100 MHz, CD_2Cl_2): δ 151.54 (*Cq* pyrazol), 137.85 (*Cq* mesityl), 137.69 (*Cq* mesityl), 135.18 (CH pyrazol), 131.73 (*Cq* mesityl), 127.88 (CH mesityl), 104.97 (CH pyrazol), 93.57 (CH olefin), 79.89 (CH_2), 70.12 (CH_2 olefin), 64.51 (CH_2), 20.95 (CH_3), 20.40 (CH_3), 15.20 (CH_3).

$\text{Tp}^{\text{Ms}}\text{Cu}(\text{cyclohexene})$ (4). Anal. Calcd for $\text{BC}_{41}\text{H}_{50}\text{N}_6\text{O}_{10}\text{Cu}$: C 70.73, H 7.07, N 11.78. Found: C 70.47, H 6.78, N 11.75. IR (KBr): $\nu(\text{B}-\text{H})$ 2449 cm^{-1} , $\nu(\text{C}=\text{C})$ 1519 cm^{-1} . ^1H NMR (400 MHz, toluene- d_8): δ 7.67 (d, $J = 2.1$ Hz, 3H), 6.70 (s, 6H), 5.87 (d, $J = 2.3$, 3H), 4.57 (s, 2H), 2.08 (s, 9H), 2.04 (s, 18H), 1.06 (m, 4H), 0.70 (m, 4H). ^{13}C NMR (100 MHz, toluene- d_8): δ 151.88 (*Cq* pyrazol), 137.73 (*Cq* mesityl), 137.18 (*Cq* mesityl), 135.60 (CH pyrazol), 132.47 (*Cq* mesityl), 127.88 (CH mesityl), 104.87 (CH pyrazol), 99.04 (CH olefin), 25.35 (CH_2), 22.40 (CH_2), 20.90 (CH_3), 20.50 (CH_3).

$\text{Tp}^{\text{Ms}}\text{Cu}(\text{styrene})$ (5). Anal. Calcd for $\text{BC}_{41}\text{H}_{50}\text{N}_6\text{O}_{10}\text{Cu}$: C 71.39, H 6.53, N 11.35. Found: C 71.34, H 6.66, N 10.92. IR (KBr): $\nu(\text{B}-\text{H}) = 2433$ cm^{-1} , $\nu(\text{C}=\text{C}) = 1513$ cm^{-1} . ^1H NMR (400 MHz, C_6D_6): δ 7.65 (d, $J = 2.1$ Hz, 3H), 6.64 (s, 6H), 5.86 (d, $J = 2.3$, 3H), 5.18 (dd, $J = 15.3$, 9.4 Hz, 1H), 3.75 (d, $J = 9.5$, 1H *cis*), 3.56 (d, $J = 15.2$ Hz, 1H *trans*), 2.05 (s, 9H), 2.00 (s, 18H). ^{13}C NMR (100 MHz, C_6D_6): δ 151.95 (*Cq* pyrazol), 137.55 (*Cq* mesityl), 137.29 (*Cq* mesityl), 135.51 (CH pyrazol), 131.78 (*Cq* mesityl), 127.98 (CH mesityl), 105.23 (CH pyrazol), 98.04 (CH olefin), 77.89 (CH_2 olefin), 21.00 (CH_3), 20.40 (CH_3).

Activation Barriers for Styrene Rotation in 5. The activation barrier for styrene rotation in **5** was calculated using the following partial ^1H NMR data (toluene- d_8 , 193 K): δ 6.65 (s, 3, aromatic mesityl-CH), 6.33 (s, 3, aromatic mesityl-CH).

Coalescence of these peaks at δ 6.51 ($\Delta\nu = 129.43$ Hz, $T_c = 233$ K) corresponds to an activation barrier of $\Delta G^\ddagger = 10.9(3)$ kcal mol⁻¹ at 233 K.

Olefin Exchange Reactions. One equivalent of olefin-R² was added to a solution of Tp^{M_s}Cu(olefin-R¹) in 0.6 mL of deuterated solvent, and the solution was transferred to an NMR tube that was sealed with a Teflon stopper. The reaction mixture was monitored every hour at room temperature until an equilibrium mixture was reached. Accounting for the relative concentrations of olefin-R¹ and olefin-R² in solution afforded the equilibrium constant K_{eq} at room temperature for the exchange reaction below.



Kinetic Study of the Exchange Reaction of Tp^{M_s}Cu(aee), 3, with 1-Hexene. At 0 °C, 1, 2, 3, 4, and 5 equiv of 1-hexene (from a stock 1.6 M solution in CD₂Cl₂) were added to five solutions of 10 mg of Tp^{M_s}Cu(aee) (0.02 M) in 0.7 mL of CD₂Cl₂. The reaction was monitored by ¹H NMR until the equilibrium was reached. The k_{obs} at different olefin concentrations were obtained by first-order linear plots of $\ln([3]_e/[3] - [3]_e)$ vs time (see Supporting Information).

Reaction of Allyl Ethyl Ether and EDA Catalyzed by Tp^{M_s}Cu-(THF). A solution of ethyl diazoacetate (0.114 g, 1 mmol) in 10 mL of 1,2-dichloroethane was added to a solution of Tp^{M_s}Cu-(THF) (8.6 mg, 0.0125 mmol) and allyl ethyl ether (0.76 g, 8.8 mmol) in 10 mL of 1,2-dichloroethane. The reaction mixture was heated at 70 °C. The consumption of EDA was monitored by IR. After 24 h, volatiles were removed under vacuum and the reaction crude was analyzed by ¹H NMR spectroscopy. The products have been identified by comparison with data previously reported.^{37–39} The addition of 1,4-dimethoxybenzene as internal reference provided both mass balance, referred to initial EDA, and the ratio of products formed in each transformation. Purification of products was performed with neutral silica gel as described previously.⁵

X-ray Crystal Structure Analyses of 1, 2, and 4. A single crystal, of each representative compound, of suitable size was mounted on a glass fiber using perfluoropolyether oil (FOMBLIN 140/13, Aldrich) in the cold N₂ stream of a low-temperature device attachment. Full crystallographic data and structure refinement are given in the Supporting Information. Intensity data were performed on a Bruker-AXS X8 Kappa diffractometer equipped with an Apex-II CCD area detector, using a graphite monochromator Mo K α_1 ($\lambda = 0.71073$ Å) and a Bruker Cryo-Flex low-temperature device. The data collection strategy used in all instances was phi and omega scans with narrow frames. Instrument and crystal stability were evaluated from the measurement of equivalent reflections at different measuring times, and no decay was observed. The data were reduced (SAINT)⁴⁰ and corrected for Lorentz and polarization effects, and a semiempirical absorption correction was applied (SADABS).⁴¹ The structure was solved by direct methods (SIR-2002)⁴² and refined against all F^2 data by full-matrix least-squares techniques

(37) Doyle, M. P.; Hu, W. *J. Org. Chem.* **2000**, *65*, 8839–8847.

(38) Hekking, K. F. W.; Waalboer, D. C. J.; Moleands, M. A. M.; Delft, F. J.; Rutges, F. P. J. *T. J. Adv. Synth. Catal.* **2007**, *305*, 95–106.

(39) Clark, J. S.; Fessard, T. C.; Whitlock, G. A. *Tetrahedron* **2006**, *62*, 73–78.

(40) SAINT+, Bruker-APEX 2 package, Version 2.1; Bruker Analytical X-ray Solutions: Madison, WI, 2006.

(41) SADABS, Bruker-APEX 2 package, Version 2.1; Bruker Analytical X-ray Solutions: Madison, WI, 2006.

(42) Burla, M. C.; Camalli, M.; Carrozzini, B.; Cascarano, G. L.; Giacovazzo, C.; Polidori, G.; Spagna, R. *SIR2002*: the program. *J. Appl. Crystallogr.* **2003**, *36*, 1103

(43) SHELXTL 6.14; Bruker AXS, Inc.: Madison, WI, 2000–2003.

(SHELXTL-6.14)⁴³ minimizing $w[F_o^2 - F_c^2]^2$. All non-hydrogen atoms were refined with anisotropic displacement parameters. The hydrogen atoms were introduced into geometrically calculated positions and refined riding on the corresponding parent atoms.

Crystal data for 1: C₃₈H₄₄BCuN₆, $M_w = 659.14$, colorless prism crystal of dimensions 0.19 × 0.15 × 0.08 mm³, monoclinic, space group $P\bar{1}$ (no. 2), $a = 9.1125(14)$ Å, $b = 11.1306(16)$ Å, $c = 17.644(3)$ Å, $\alpha = 102.973(5)^\circ$, $\beta = 96.970(6)^\circ$, $\gamma = 94.440(6)^\circ$, $V = 1720.9(5)$ Å³, $T = 100(2)$ K, $Z = 2$, $D = 1.272$ Mg/m³, $\rho = 0.670$ mm⁻¹, $F(000) = 696$; 38 117 reflections measured, of which 13 102 were unique ($R_{int} = 0.0502$). The asymmetric unit of the structure is formed by two equivalent but symmetrically independent complexes of 1. Refined parameters 830, final $R_1 = 0.0473$ for reflections with $I > 2\sigma(I)$, $wR_2 = 0.1052$ (all data), GOF = 1.002. Final largest diffraction peak and hole: 0.557 and -0.656 e Å⁻³.

Crystal data for 2: C₄₂H₅₂BCuN₆, $M_w = 715.25$, colorless plate crystal of dimensions 0.16 × 0.13 × 0.08 mm³, triclinic, space group $P\bar{1}$ (no. 2), $a = 9.0845(7)$ Å, $b = 12.6099(9)$ Å, $c = 17.7141(12)$ Å, $\alpha = 97.856(2)^\circ$, $\beta = 97.736(2)^\circ$, $\gamma = 102.926(2)^\circ$, $V = 1930.4(2)$ Å³, $T = 100(2)$ K, $Z = 2$, $D = 1.231$ Mg/m³, $\rho = 0.603$ mm⁻¹, $F(000) = 760$; 71 663 reflections measured, of which 11 521 were unique ($R_{int} = 0.0680$). Refined parameters 451, final $R_1 = 0.0547$ for reflections with $I > 2\sigma(I)$, $wR_2 = 0.1547$ (all data), GOF = 1.044. Final largest diffraction peak and hole: 1.073 and -1.043 e Å⁻³.

Crystal data for 4: C₄₂H₅₀BCuN₆, $M_w = 713.23$, colorless prism crystal of dimensions 0.49 × 0.47 × 0.46 mm³, orthorhombic, space group $Pna2_1$ (no. 33), $a = 16.3641(9)$ Å, $b = 11.8396(6)$ Å, $c = 19.3116(10)$ Å, $\alpha = \beta = \gamma = 90^\circ$, $V = 3741.5(3)$ Å³, $T = 100(2)$ K, $Z = 4$, $D = 1.266$ Mg/m³, $\rho = 0.622$ mm⁻¹, $F(000) = 1512$; 87 199 reflections measured, of which 11 153 were unique ($R_{int} = 0.0341$). Refined parameters 466, final $R_1 = 0.0300$ for reflections with $I > 2\sigma(I)$, $wR_2 = 0.0778$ (all data), GOF = 1.055. Absolute structure parameter (Flack x parameter): 0.007(6). Final largest diffraction peak and hole: 0.706 and -0.544 e Å⁻³.

Computational Details. Calculations were carried out with DFT using the B3LYP functional^{44–46} as implemented in Gaussian 03.⁴⁷ The 6-31G(d) basis set^{48,49} was used for all atoms except copper, which was treated with SDD and the associated effective core potential.⁵⁰ Frequency calculations

(44) Becke, A. D. *J. Chem. Phys.* **1993**, *98*, 5648–5652.

(45) Lee, C. T.; Yang, W. T.; Parr, R. G. *Phys. Rev. B* **1988**, *37*, 785–789.

(46) Stephens, P. J.; Devlin, F. J.; Chabalowski, C. F.; Frisch, M. J. *J. Phys. Chem.* **1994**, *98*, 11623–11627.

(47) Frisch, M. J.; Trucks, G. W.; Schlegel, H. B.; Scuseria, G. E.; Robb, M. A.; Cheeseman, J. R.; Montgomery, J. A., Jr.; Vreven, T.; Kudin, K. N.; Burant, J. C.; Millam, J. M.; Iyengar, S. S.; Tomasi, J.; Barone, V.; Mennucci, B.; Cossi, M.; Scalmani, G.; Rega, N.; Petersson, G. A.; Nakatsuji, H.; Hada, M.; Ehara, M.; Toyota, K.; Fukuda, R.; Hasegawa, J.; Ishida, M.; Nakajima, T.; Honda, Y.; Kitao, O.; Nakai, H.; Klene, M.; Li, X.; Knox, J. E.; Hratchian, H. P.; Cross, J. B.; Bakken, V.; Adamo, C.; Jaramillo, J.; Gomperts, R.; Stratmann, R. E.; Yazyev, O.; Austin, A. J.; Cammi, R.; Pomelli, C.; Ochterski, J. W.; Ayala, P. Y.; Morokuma, K.; Voth, G. A.; Salvador, P.; Dannenberg, J. J.; Zakrzewski, V. G.; Dapprich, S.; Daniels, A. D.; Strain, M. C.; Farkas, O.; Malick, D. K.; Rabuck, A. D.; Raghavachari, K.; Foresman, J. B.; Ortiz, J. V.; Cui, Q.; Baboul, A. G.; Clifford, S.; Cioslowski, J.; Stefanov, B. B.; Liu, G.; Liashenko, A.; Piskorz, P.; Komaromi, I.; Martin, R. L.; Fox, D. J.; Keith, T.; Al-Laham, M. A.; Peng, C. Y.; Nanayakkara, A.; Challacombe, M.; Gill, P. M. W.; Johnson, B.; Chen, W.; Wong, M. W.; Gonzalez, C.; Pople, J. A. *Gaussian 03*, Revision C.02; Gaussian, Inc.: Wallingford, CT, 2004.

(48) Francl, M. M.; Pietro, W. J.; Hehre, W. J.; Binkley, J. S.; Gordon, M. S.; Defrees, D. J.; Pople, J. A. *J. Chem. Phys.* **1982**, *77*, 3654–3665.

(49) Hehre, W. J.; Ditchfield, R.; Pople, J. A. *J. Chem. Phys.* **1972**, *56*, 2257–2261.

(50) Andrae, D.; Haussermann, U.; Dolg, M.; Stoll, H.; Preuss, H. *Theor. Chim. Acta* **1990**, *77*, 123–141.

were performed to characterize the stationary points as minima. Free energy corrections were introduced for a pressure of 1 atm and a temperature of 298 K.

Acknowledgment. We thank the MICINN (Proyecto CTQ2008–00042BQU, CTQ2008-06866-CO2-02/BQU and Consolider Ingenio 2010 grant CSD2006-0003), the Junta de Andalucía (Proyecto P07-FQM-02794), and the

ICIQ Foundation for financial support. C.M. thanks the Ministerio de Educación for a research fellowship.